

# Antitumor Active Platinum Blue Complexes: Syntheses and Solution Behaviors of 3,3-Dimethylglutarimide- and Glutarimide-Bridged Platinum Blue Complexes and Their Reactions with 5'-Guanosine Monophosphate

Jun Matsunami, Hiroshi Urata, and Kazuko Matsumoto\*

Department of Chemistry, Waseda University, Tokyo 169, Japan

Received March 18, 1994<sup>⊗</sup>

Syntheses and solution behaviors of antitumor active glutarimide (GI)- and 3,3-dimethylglutarimide (DMGI)-bridged platinum blues,  $[\text{Pt}_4(\text{NH}_3)_8(\text{GI})_4](\text{NO}_3)_5 \cdot 2\text{H}_2\text{O}$  (**1**) and  $[\text{Pt}_4(\text{NH}_3)_8(\text{DMGI})_4](\text{NO}_3)_5 \cdot 2\text{H}_2\text{O}$  (**2**), are reported. Compounds **1** and **2** were characterized by elemental analysis, cyclic-voltammetry, and ESR spectroscopy and were found to be basically identical to previously reported tetranuclear platinum blue complexes: both compounds exhibit an irreversible wave at 0.725 and 0.763 V vs SCE, respectively. Compound **2** shows an axial pattern ESR spectrum with  $g_{\perp} = 2.36$  and  $g_{\parallel} = 1.992$ .  $^1\text{H}$  and  $^{195}\text{Pt}$  NMR spectroscopy of **1** revealed that the tetranuclear complex is not stable in aqueous solution: it is first reduced by water to a head-to-head (HH) isomer of  $[\text{Pt}_2(\text{NH}_3)_4(\text{GI})_2]^{2+}$  (**10**) following the equation,  $1 + \frac{1}{2}\text{H}_2\text{O} \xrightarrow{k_1} 2 \times 10 + \frac{1}{4}\text{O}_2 + \text{H}^+$ , with a first-order rate constant of  $k_1 = 2.81 (1) \times 10^{-3} \text{ s}^{-1}$ . Compound **10** further undergoes disruptive reaction to form monomers, *cis*- $[\text{Pt}(\text{NH}_3)_2(\text{GI})_2]$  (**12**) and *cis*- $[\text{Pt}(\text{NH}_3)_2(\text{OH}_2)_2]^{2+}$  (**8**). Part of **10** isomerizes to the head-to-tail isomer **11**, which then disrupts to *cis*- $[\text{Pt}(\text{NH}_3)_2(\text{GI})(\text{OH}_2)]^+$  (**13**). Similar reactions occur to another platinum blue **2**, but HH to HT isomerization is hindered in this case. It seems that the antitumor activity of these platinum blue compounds stems from the decomposition product *cis*- $[\text{Pt}(\text{NH}_3)_2(\text{H}_2\text{O})_2]$  (**8**), which is also produced from the famous antitumor drug *cis*- $\text{PtCl}_2(\text{NH}_3)_2$  in solution, and reacts with DNA to exhibit the activity. Reaction of **1** with 5'-guanosinemonophosphate (5'-GMP) produces *cis*- $[\text{Pt}(\text{NH}_3)_2(5'\text{-GMP})_2]$  (**17**), which also strongly supports the activity mechanism of the platinum blue compounds is the same for *cis*- $\text{PtCl}_2(\text{NH}_3)_2$ .

## Introduction

"Platinum blue" was first found in the hydrolysis reaction of *cis*- $\text{PtCl}_2(\text{CH}_3\text{CN})_2$ , and was first formulated as  $\text{Pt}(\text{II})(\text{CH}_3\text{-CONH}_2)_2 \cdot \text{H}_2\text{O}$ ,<sup>1</sup> but the formula and the structure have been controversial<sup>2</sup> until modern times, since the reported synthetic method was not reproducible and the reliable crystal structure analysis was not reported. These compounds reattracted chemist's attention again when the antitumor active *cis*- $\text{PtCl}_2(\text{NH}_3)_2$  (*cis*-DDP) was found to exhibit its activity by reacting with DNA bases.<sup>3–8</sup> Researchers found, in an attempt to identify the reaction products of *cis*-DDP with DNA bases, that the platinum compound reacts with pyrimidines to produce dark blue compounds, "platinum pyrimidine blues", and what is more intriguing is that these blue compounds also exhibit antitumor activity against S180.<sup>9</sup> This activity was, however, not fully pursued at that time because the synthetic method for the blue compounds lacked reproducibility, and presumably also because the high optimal dose level of these compounds and their companion immunogenicity made them less promising as

practical chemotherapeutic reagents. Although, after about a decade, several groups again reported antitumor activities and preparative procedures for platinum blues that are different from the previous ones,<sup>10,11</sup> the mechanistic study of the antitumor activities of platinum blues did not make any progress, since they still seem to lack reliable formulas or they may be mixtures, and the structures are not known.

The breakthrough in the chemistry of platinum blues was the first X-ray structural study of  $\alpha$ -pyridonate-bridged platinum blue,  $[\text{Pt}_4(\text{NH}_3)_8(\text{C}_5\text{H}_4\text{NO})_4](\text{NO}_3)_5 \cdot 2\text{H}_2\text{O}$ .<sup>12–14</sup> The complex cation turned out to be a mixed-valent Pt(II,III) tetranuclear compound with a platinum chain structure, but its significance to the antitumor activity has still been unknown, because structurally-elucidated  $\alpha$ -pyridonate-bridged blue is antitumor inactive,<sup>15</sup> while the active blue compounds so far reported have not been structurally elucidated.

We have recently isolated the antitumor active title compounds, whose structures have been solved by X-ray diffraction analysis,<sup>16</sup> and have found very important solution behavior, which is closely related to the mechanism of the antitumor activity. The solution behaviors of several antitumor active and

\* Abstract published in *Advance ACS Abstracts*, November 15, 1994.

- (1) Hofmann, K. A.; Bugge, G. *Ber.* **1908**, *41*, 312.
- (2) (a) Gillard, R. D.; Wilkinson, G. *J. Chem. Soc.* **1964**, 2835. (b) Brown, D. B.; Robin, M. B.; Burbank, R. D. *J. Am. Chem. Soc.* **1968**, *90*, 5621. (c) Brown, D. B.; Burbank, R. D.; Robin, M. B. *J. Am. Chem. Soc.* **1969**, *91*, 2895.
- (3) Rosenberg, B.; Van Camp, L.; Krigas, T. *Nature (London)* **1965**, *205*, 698.
- (4) Rosenberg, B.; Van Camp, L.; Trosko, J. E.; Mansour, V. H. *Nature (London)* **1969**, *222*, 385.
- (5) Rosenberg, B.; Van Camp, L. *Cancer Res.* **1970**, *30*, 1799.
- (6) Sherman, S. E.; Lippard, S. J. *Chem. Rev.* **1987**, *87*, 1153.
- (7) Sundquist, W. I.; Lippard, S. J. *Coord. Chem. Rev.* **1990**, *100*, 293.
- (8) Reedijk, J. *Pure Appl. Chem.* **1987**, *59*, 181.
- (9) (a) Davidson, J. P.; Faber, P. J.; Fischer, R. G., Jr.; Mansy, S.; Peresie, H. J.; Rosenberg, B.; Van Camp, L. *Cancer Chemother. Rep.* **1975**, *59*, 287. (b) Rosenberg, B. *Cancer Chemother. Rep.* **1975**, *59*, 589.

- (10) Arrizabalaga, P.; Castan, P.; Laurent, J.-P.; Cros, S.; Francois, G. *Eur. J. Med. Chem.* **1984**, *19*, 501.
- (11) Okuno, Y.; Tonosaki, K.; Inoue, T.; Yonemitsu, O.; Sasaki, T. *Chem. Lett.* **1986**, 1947.
- (12) (a) Barton, J. K.; Rabinowitz, H. N.; Szalda, D. J.; Lippard, S. J. *J. Am. Chem. Soc.* **1977**, *99*, 2827. (b) Barton, J. K.; Szalda, D. J.; Rabinowitz, H. N.; Waszczak, J. V.; Lippard, S. J. *J. Am. Chem. Soc.* **1979**, *101*, 1434.
- (13) Barton, J. K.; Best, S. A.; Lippard, S. J.; Walton, R. A. *J. Am. Chem. Soc.* **1978**, *100*, 3785.
- (14) Barton, J. K.; Caravana, C.; Lippard, S. J. *J. Am. Chem. Soc.* **1979**, *101*, 7269.
- (15) Matsumoto, K. Unpublished result.
- (16) Matsumoto, K.; Matsunami, J.; Urata, H. *Chem. Lett.* **1993**, 597.

inactive platinum blue and related compounds are compared and are discussed with regard to their activities. The reactions of the antitumor active platinum blue compounds with 5'-guanosine monophosphate (5'-GMP) are also reported. Preliminary result of the present study has been published elsewhere.<sup>16</sup>

### Experimental Section

**Preparation of the Platinum Complexes.** A platinum blue compound with glutarimide (GI) ligand,  $[\text{Pt}_4(\text{NH}_3)_8(\text{GI})_4](\text{NO}_3)_5 \cdot 2\text{H}_2\text{O}$  (**1**), was prepared as follows. To a solution of *cis*- $[\text{Pt}(\text{NH}_3)_2(\text{OH}_2)_2]^{2+}$  (1 mmol in 10 mL of  $\text{H}_2\text{O}$ ), which was prepared by adding 2 equiv of  $\text{AgNO}_3$  to *cis*- $\text{PtCl}_2(\text{NH}_3)_2$  and filtering off  $\text{AgCl}$ , was added 1 mmol of glutarimide, and the pH of the solution was adjusted to 7 with 1 M  $\text{NaOH}$ . After the solution was heated at 90 °C for 2 h, it was cooled with ice and filtered. To the filtrate 1 mL of concd  $\text{HNO}_3$  was added and the solution was left at room temperature for several days to produce blue-black crystals. Anal. Calcd for  $\text{Pt}_4\text{C}_{20}\text{H}_{52}\text{N}_{17}\text{O}_{25}$ : C, 14.04; H, 3.06; N, 13.92%. Found: C, 13.84; H, 2.91; N, 13.62%.

The platinum blue compound with 3,3-dimethylglutarimide (DMGI) ligand,  $[\text{Pt}_4(\text{NH}_3)_8(\text{DMGI})_4](\text{NO}_3)_5 \cdot 2\text{H}_2\text{O}$  (**2**), was prepared in the same way as for **1**, except that 4 mmol of 3,3-dimethylglutarimide was added instead of glutarimide. Anal. Calcd for  $\text{Pt}_4\text{C}_{28}\text{H}_{68}\text{N}_{17}\text{O}_{25}$ : C, 18.44; H, 3.73; N, 13.06%. Found: C, 18.64; H, 3.76; N, 12.96%.

The head-to-head (HH) isomer of  $[\text{Pt}(\text{II})_2(\text{NH}_3)_4(\text{DMGI})_2](\text{NO}_3)_2 \cdot \text{H}_2\text{O}$  (**3**) was obtained as pale green crystals after the filtrate of head-to-tail (HT)  $[\text{Pt}(\text{II})_2(\text{NH}_3)_4(\text{DMGI})_2](\text{NO}_3)_2 \cdot \text{H}_2\text{O}$  (**4**)<sup>17</sup> was allowed to stand at room temperature for several days. Anal. Calcd for  $\text{Pt}_2\text{C}_{14}\text{H}_{34}\text{N}_8\text{O}_{11}$ : C, 19.09; H, 3.89; N, 12.73%. Found: C, 18.90; H, 3.87; N, 12.60%.

*cis*- $[\text{Pt}(\text{NH}_3)_2(\text{DMGI})_2]$  (**5**) was prepared as follows. To a solution of *cis*- $[\text{Pt}(\text{NH}_3)_2(\text{OH}_2)_2]^{2+}$  (1 mmol in 10 mL of  $\text{H}_2\text{O}$ ) was added 2 mmol of 3,3-dimethylglutarimide, and the pH of the solution was adjusted to 5 with 0.1 M  $\text{NaOH}$ . After the solution was heated at 80 °C for 2.5 h in the dark, it was cooled to room temperature and was evaporated to give yellow precipitate of **5**. It was filtered and was recrystallized from water. Anal. Calcd for  $\text{PtC}_{14}\text{H}_{26}\text{N}_4\text{O}_4$ : C, 33.00; H, 5.15; N, 11.00%. Found: C, 33.25; H, 5.12; N, 10.89%.

Compound **4**,<sup>17</sup>  $\alpha$ -pyrrolidonate-bridged platinum tan  $[\text{Pt}_4(\text{NH}_3)_8(\text{C}_4\text{H}_6\text{NO})_4](\text{NO}_3)_6 \cdot 2\text{H}_2\text{O}$  (**6**),<sup>18</sup> and acetamidate-bridged platinum blue  $[\text{Pt}_8(\text{NH}_3)_{16}(\text{CH}_3\text{CONH})_8](\text{NO}_3)_{10} \cdot 4\text{H}_2\text{O}$  (**7**),<sup>19,20</sup> were prepared according to the reported procedures.

**Antitumor Screening Test.** The antitumor activities were examined as follows.  $\text{BDF}_1$  mice were inoculated ip with  $10^6$  L1210 cells (day 0) and were treated ip with the dose of the test complex on days 1, 5, and 9. Mean survival times (MST) of six treated mice and six control tumor-bearing mice were calculated and the %T/C values were determined as %T/C = MST (treated)/MST (control).

**NMR Measurements.**  $^1\text{H}$  NMR spectra were acquired on a JEOL JNM EX 270WB or a GE Omega 500 spectrometer and all the chemical shifts were measured relative to TSP- $d_4$ .  $^{195}\text{Pt}$  NMR measurements were run on a GE Omega 500 spectrometer operating at 107.30 MHz with a 5 mm tunable probe (90° pulse is 14.5  $\mu\text{s}$ ). Spectral data were acquired with 70° pulse, 200 kHz spectral width, and 4 K data points. Chemical shifts were measured relative to  $\text{K}_2\text{PtCl}_4$  in  $\text{D}_2\text{O}$ , which was used as an external reference (-1624 ppm vs  $\text{Na}_2\text{PtCl}_6$  in  $\text{D}_2\text{O}$ ). All the chemical shifts are expressed positive to lower shielding.

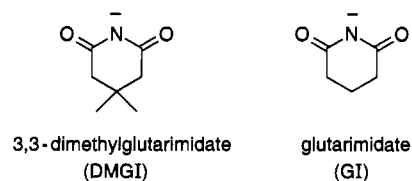
**Physical Measurements.** ESR spectra were recorded on a JEOL JES-RE2X X-band spectrometer operating at  $3000 \pm 1500$  G with the microcrystalline samples. UV-vis spectra were recorded on a Shimadzu UV-260 spectrophotometer. For kinetic study, a Shimadzu UV-160A was also used. The electrochemical measurements were performed on a Fuso 315A potentiostat with a glassy carbon disk working electrode and a platinum wire as a counterelectrode. All of the measurements were carried out in 0.5 M  $\text{H}_2\text{SO}_4$  with a three-electrode system by using SCE as a reference electrode.

**Table 1.** Antitumor Activities of Platinum Compounds against L1210 *in vivo*

| Complex   | dose (mg/kg) | %T/C           |
|---|--------------|----------------|
| glutarimide blue,<br>$[\text{Pt}_4(\text{NH}_3)_8(\text{GI})_4](\text{NO}_3)_5 \cdot 2\text{H}_2\text{O}$ ( <b>1</b> )                              | 50           | 102            |
|   | 26           | 164            |
|   | 12.5         | 139            |
| 3,3-dimethylglutarimide blue,<br>$[\text{Pt}_4(\text{NH}_3)_8(\text{DMGI})_4](\text{NO}_3)_5 \cdot 2\text{H}_2\text{O}$ ( <b>2</b> )                | 50           | 131            |
|   | 25           | 156            |
|   | 12.5         | 200            |
|   | 6.25         | 132            |
| 3,3-Dimethylglutarimide HH dimer,<br>$[\text{Pt}_2(\text{NH}_3)_4(\text{DMGI})_2](\text{NO}_3)_2 \cdot \text{H}_2\text{O}$ ( <b>3</b> )             | 3.12         | 114            |
|   | 50           | 0 <sup>a</sup> |
|   | 25           | 133            |
| 3,3-dimethylglutarimide HT dimer,<br>$[\text{Pt}_2(\text{NH}_3)_4(\text{DMGI})_2](\text{NO}_3)_2 \cdot \text{H}_2\text{O}$ ( <b>4</b> )             | 12.5         | 140            |
|   | 6.25         | 162            |
|   | 3.12         | 125            |
|   | 1.56         | 111            |
| $\alpha$ -pyrrolidone tan,<br>$[\text{Pt}_4(\text{NH}_3)_8(\text{C}_4\text{H}_6\text{NO})_4](\text{NO}_3)_6 \cdot 2\text{H}_2\text{O}$ ( <b>6</b> ) | 50           | 98             |
|   | 25           | 93             |
|   | 12.5         | 90             |
| acetamide blue,<br>$[\text{Pt}_8(\text{NH}_3)_{16}(\text{C}_2\text{H}_4\text{NO})_8](\text{NO}_3)_{10} \cdot 4\text{H}_2\text{O}$ ( <b>7</b> )      | 50           | 102            |
|   | 25           | 107            |
|   | 12.5         | 110            |
| <i>cis</i> -DDP <sup>b</sup><br>$[\text{PtCl}_2(\text{NH}_3)_2]$  | 50           | 102            |
|   | 25           | 202            |
|   | 12.5         | 278            |
|   | 6.25         | 220            |
|   | 3.12         | 200            |

<sup>a</sup> %T/C value of 0 means that more than three mice died before day 5. <sup>b</sup> %T/C values for *cis*-DDP were taken from ref 21.

### Scheme 1



### Results and Discussion

**Antitumor Screening Results of the Platinum Complexes.** Table 1 summarizes the results of the antitumor screening test for the platinum blue and related complexes. Complexes **1** and **2** has the activity comparable to that of *cis*-DDP, while another tetranuclear complex (**6**) is inactive. Dinuclear HH isomer with DMGI ligand **3** (Scheme 1), is also active, whereas its HT isomer **4** is inactive. Octanuclear acetamidate-bridged complex **7** is also inactive. These results show that the antitumor activity varies even among complexes with a same ligand but with different structures or different Pt oxidation states.

**Chemical Properties of DMGI-Bridged Platinum Blue Complex 2.** Crystal structure of **2** has already been published elsewhere<sup>16</sup> and the tetranuclear mixed-valent structure has been confirmed to be similar to those of the previously reported platinum blue complexes.<sup>12,22</sup> Figure 1 shows the ESR spectra of **2** in solid state and in solution, which indicates that **2** is not stable in solution. Actually the solution becomes ESR silent after a day. The hyperfine structure of **2** is similar to those of other platinum blue complexes,<sup>13,14,27</sup> indicating that the one unpaired electron is delocalized over the four platinum atoms. However, the relative abundance of the electron on each platinum atom could not be determined, since the usual theoretical calculation for the relative intensity by assuming various hyperfine coupling constants for the four platinum atoms

(17) Urata, H.; Moriyama, H.; Matsumoto, K. *Inorg. Chem.* **1991**, *30*, 3914.

(18) (a) Matsumoto, K.; Fuwa, K. *J. Am. Chem. Soc.* **1982**, *104*, 897. (b) Matsumoto, K.; Takahashi, H.; Fuwa, K. *Inorg. Chem.* **1983**, *22*, 4086.

(19) Sakai, K.; Matsumoto, K. *J. Am. Chem. Soc.* **1989**, *111*, 3074.

(20) Matsumoto, K.; Sakai, K.; Nishio, K.; Tokisue, Y.; Ito, R.; Nishide, T.; Shichi, Y. *J. Am. Chem. Soc.* **1992**, *114*, 8110.

(21) Connors, T. A.; Roberts, J. J. *Platinum Coordination Complexes in Cancer Chemotherapy Recent Results Cancer Res.* **1974**, *48*.

(22) O'Halloran, T. V.; Mascharak, P. K.; Williams, I. D.; Roberts, M. M.; Lippard, S. J. *Inorg. Chem.* **1987**, *26*, 1261.

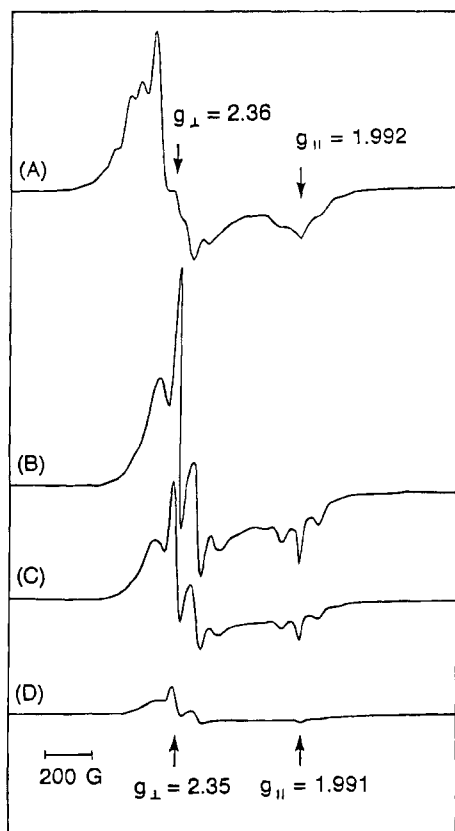


**Figure 1.** ESR spectra of **2**: (A) solid sample (at room temperature), B–D **2** 3 mM solution in 0.5 M H<sub>2</sub>SO<sub>4</sub> at 77 K; (B) 10 min, (C) 120 min, (D) 240 min after dissolution.

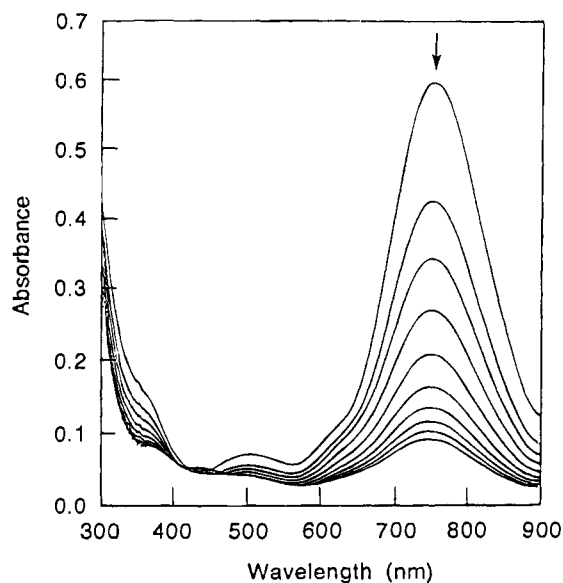


**Figure 2.** UV-vis spectra of **2** in 0.1 mM H<sub>2</sub>SO<sub>4</sub>. The spectrum was measured every 10 min after dissolution.

did not give any satisfactory result for the observed relative hyperfine intensities, 0.2:4:13:24:58:68:100. The optimum calculated result was obtained when the hyperfine coupling constants for the outer two Pt atoms is twice that of the inner Pt atoms, and the calculated intensities were 0.3:3:3:8:22:48:62:100. The UV-vis spectra of **2** is shown in Figure 2 as a function of time. The absorptions at 752 and 490 nm decrease after dissolution. The cyclic voltammogram of **2** shows a pair of irreversible redox waves at 0.763 V ( $= (E_{pc} + E_{pa})/2$ ,  $E_{pc} = 0.715$  V,  $E_{pa} = 0.810$  V) vs SCE. The cyclic voltammogram of **1** shows a pair of irreversible wave at 0.725 V ( $= (E_{pc} + E_{pa})/2$ ,  $E_{pc} = 0.685$  V,  $E_{pa} = 0.765$  V).

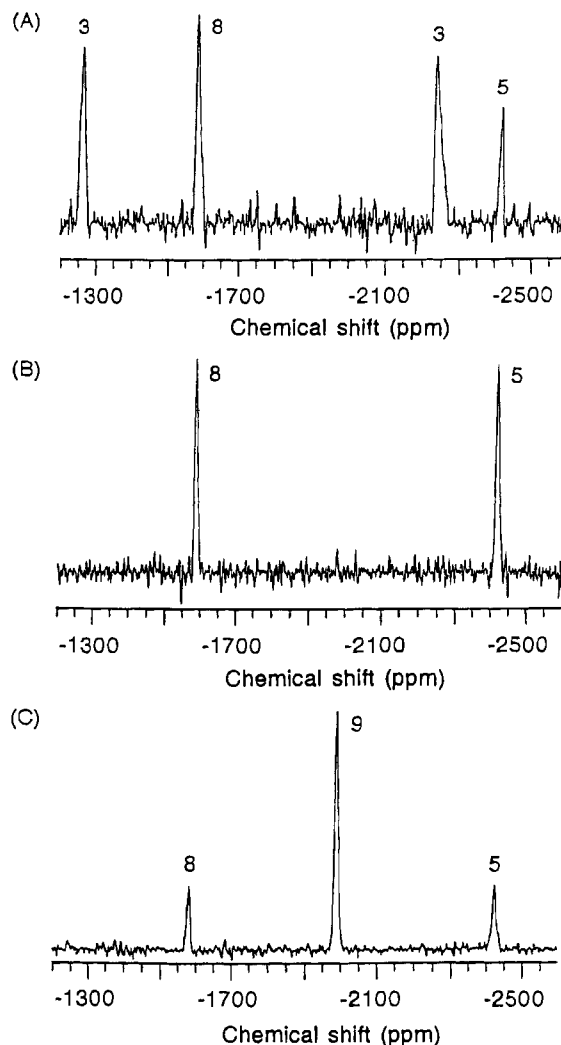


**Figure 3.** <sup>195</sup>Pt NMR spectra of **3** in H<sub>2</sub>O: (A) after dissolution, (B) after 3 days, (C) after 30 days. The resonances are assigned as follows: **3** –1259, –2233 ppm; **5** –2423 ppm; **8** –1581 ppm; **9** –1988 ppm. The chemical shifts are relative to K<sub>2</sub>PtCl<sub>4</sub> in D<sub>2</sub>O at –1624 ppm.

#### Solution Behavior of Platinum Blue Complexes **1** and **2**.

In order to understand why some tetranuclear complexes in Table 1 are antitumor active while others are not, the chemical species actually present in the solution were examined with <sup>195</sup>Pt NMR spectroscopy. Since **2** does not dissolve in water in sufficient amount for <sup>195</sup>Pt NMR study, its reduced form **3** was measured. Figure 3 shows <sup>195</sup>Pt NMR spectra of **3** in H<sub>2</sub>O just after dissolution (A), after 3 days (B), and after 30 days (C). The assignment of the signals in Figure 3 was made referenced to the spectra of isolated **5** and *cis*-[Pt(NH<sub>3</sub>)<sub>2</sub>(OH<sub>2</sub>)<sub>2</sub>]<sup>2+</sup> (**8**), and also to the reported <sup>195</sup>Pt NMR chemical shifts of the analogous platinum complexes with α-pyridonate and other related ligands.<sup>23</sup> It turns out from Figure 3 that **3** produces dimeric and monomeric species after dissolution. Figure 3(A) shows that a monomer with DMGI ligand **5** and a diaqua compound **8** are produced from **3** after dissolution, which indicates that isomerization of HH dimer **3** to the HT dimer, as reported for α-pyridonate-<sup>26</sup> or α-pyrrolidonate<sup>28</sup>-bridged dimers, has not occurred, and that HH dimer **3** undergoes hydrolysis to **5** and **8**. After 3 days, only **5** and **8** are observed, both of which then gradually react to form *cis*-[Pt(NH<sub>3</sub>)<sub>2</sub>(DMGI)(OH<sub>2</sub>)<sub>2</sub>]<sup>+</sup> (**9**) (<sup>195</sup>Pt chemical shift is –1988 ppm). Figure 3 shows that diamagnetic HH dimer **3** undergoes solvolysis to give **5** and **8**, which gradually react to give **9**. Although <sup>195</sup>Pt NMR spectrum of

(23) Hollis, L. S.; Lippard, S. J. *J. Am. Chem. Soc.* **1983**, *105*, 3494.

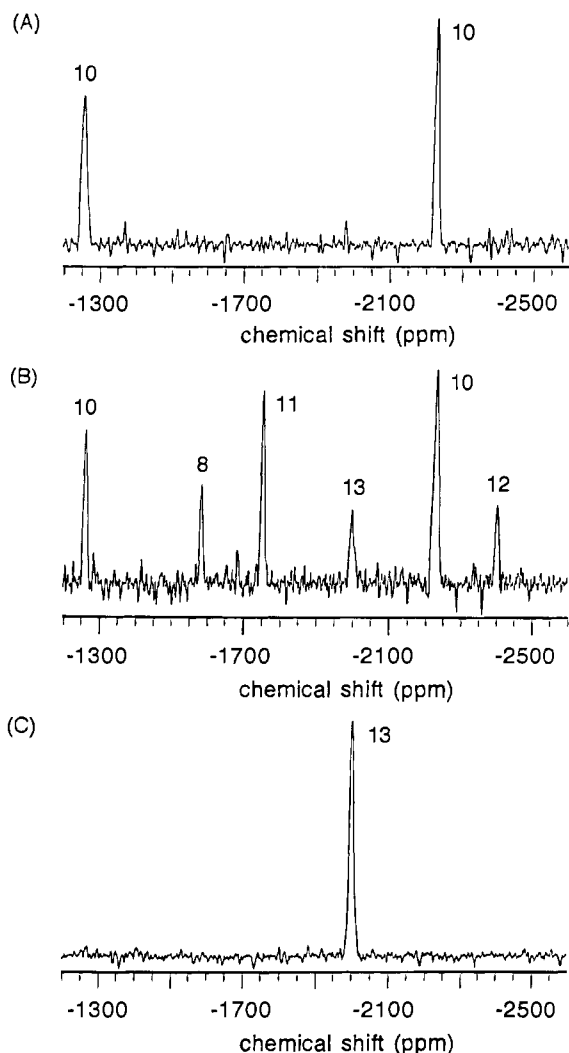


**Figure 4.**  $^{195}\text{Pt}$  NMR spectra of **1** in  $\text{H}_2\text{O}$ : (A) after dissolution, (B) after 1 days, (C) after 10 days. The resonances are assigned as follows: **8** –1581 ppm; **10** –1260, –2223 ppm; **11** –1749 ppm; **12** –2408 ppm; **13** –1996 ppm. The chemical shifts are relative to  $\text{K}_2\text{PtCl}_4$  in  $\text{D}_2\text{O}$ .

tetranuclear blue complex **2** could not be measured, because of its low solubility in  $\text{H}_2\text{O}$ ,  $^1\text{H}$  NMR spectroscopy confirmed that both **2** and **3** show the same spectrum (Figure S1) in  $\text{D}_2\text{O}$ , which means that **2** is reduced by  $\text{H}_2\text{O}$  to **3** and then changes to monomers in exactly the same way as **3**. Similar reduction of a tetranuclear blue complex by water to an amidate-bridged Pt(II) dimer complex has already been reported for  $\alpha$ -pyrrolidone-bridged blue compound, where water is oxidized to  $\text{O}_2$ .<sup>24</sup>

$^{195}\text{Pt}$  NMR spectra of **1** in  $\text{H}_2\text{O}$  are shown in Figure 4. The assignment of the signals in the figures was based on the spectra of the analogous compound **3** (Figure 3) and also on the reported  $^{195}\text{Pt}$  chemical shifts of the amidate-coordinated platinum complexes.<sup>28</sup> When **1** is dissolved in  $\text{H}_2\text{O}$ , only HH dimer  $[\text{Pt}_2(\text{NH}_3)_4(\text{GI})_2]^{2+}$  (**10**) is observed (Figure 4(A)), indicating that no isomerization to the HT isomer takes place on reduction of **1**. After 1 day, HH dimer **10**, HT dimer  $[\text{Pt}_2(\text{NH}_3)_4(\text{GI})_2]^{2+}$  (**11**), monomeric complexes *cis*- $[\text{Pt}(\text{NH}_3)_2(\text{GI})_2]$  (**12**), *cis*- $[\text{Pt}(\text{NH}_3)_2(\text{GI})(\text{OH}_2)]^+$  (**13**), and diaqua complex **8** are observed, which indicates that HH to HT isomerization takes place, and both isomers are hydrolyzed to monomeric species. After 10 days, however, the  $^{195}\text{Pt}$  NMR spectrum shows only a single peak ascribed to **13**. The reaction of **8** with **12** to produce **13** is much faster for the GI complex, compared to the correspond-

ing reaction of the DMGI complex **5**. This difference is caused by the stronger donating nature of the N atom in DMGI than that in GI. The stronger donation of DMGI is reflected also in the  $^{195}\text{Pt}$  NMR chemical shifts of **5** and **12**. The former compound has a chemical shift of –2423 ppm in  $\text{H}_2\text{O}$ , which is 15 ppm higher-field shifted than the corresponding value (–2408 ppm) of **12**. From these  $^{195}\text{Pt}$  NMR measurements, the reduction and disruption reactions of the mixed-valent tetranuclear blue complexes **1** and **2** into Pt(II) dimers and monomers are revealed, which are shown in Figure 5. The tetranuclear glutarimide-bridged complex **1** is rapidly reduced by water to HH Pt(II) dimer **10** on dissolution in water (path A). Some of the HH dimer **10** isomerizes to the HT dimer **11** (path B), which then is disrupted to monomeric species **13** (path D). Path D has already been reported for isolated HT complex **4**.<sup>17</sup> Compound **10** is partly disrupted to monomers **8** and **12** (path C). The tetranuclear 3,3-dimethylglutarimide-bridged complex **2** behaves similarly to **1**; however, only HH dimer **3** is observed and no isomerization to the HT dimer takes place in this case. Therefore, the disruptive reaction of the HH dimer **3** to monomers takes only path C, and the monomers thus produced (**5** and **8**) then react with each other to produce **9** (path E). With DMGI ligand no isomerization between HH and HT takes place, which is very different from what is so far reported for the analogous to  $\alpha$ -pyridonate- or  $\alpha$ -pyrrolidone-bridged Pt(II) dimers.<sup>25,26,28</sup> The latter compounds exhibit in aqueous solution the isomerization between the two isomeric forms, and no solvolytic disruption of the dimers into monomers is observed. These dimer to monomer disruptions are probably caused by the weaker donating ability to the N and O atoms in both GI and DMGI ligands, compared to those of  $\alpha$ -pyridonate and  $\alpha$ -pyrrolidone. The free carbonyl group not participating in the platinum coordination withdraws electron from the adjacent amide group, thus lowering the donating ability of the ligand. Unlike GI-bridged HH dimer **10**, DMGI-bridged HH dimer **3** does not show isomerization to the HT dimer, which is probably due to the bulkiness of the DMGI ligand. The isomerization is believed to proceed via Pt–N(amidate) bond cleavage and pivoting of the ligand around the Pt–O(amidate) bond.<sup>25,26</sup> For such a process, bulky DMGI ligand would be unfavorable and would hinder the isomerization reaction. In accordance with this restricted movement of the DMGI ligand,  $^1\text{H}$  NMR signal of the methyl groups in **5** is observed as a broad peak at room temperature, which separates into two peaks on lowering the temperature to 4 °C (Figure S2). This spectral behavior indicates that free rotation of the coordinated ligand around the Pt–N(amidate) bond is restricted at lower temperature. The two peaks correspond to the two methyl groups located inside and outside of the N(DMGI)–Pt–N(DMGI) angle of **5**.

**Kinetic Study for the Disruption of the Tetranuclear Compounds.** The reaction rate for path A in Figure 5 was determined with UV-vis spectrometry. Since compound **2** is sparingly soluble in water, only compound **1** was measured (Figure S3). The absorbance decrease at  $\lambda_{\text{max}}$  of 762 nm was plotted every 20 s, which was found to obey a simple first-order decay according to eq 1 with the rate constant of  $k_1 = 2.81(1) \times 10^{-3} \text{ s}^{-1}$ .

Reduction of a tetranuclear blue or tan compound by water to HH Pt(II) dimer complex accompanied by  $\text{O}_2$  production has been reported for **6**.<sup>24,27</sup> In spite of the successive reactions (paths B and C), reaction **1** is observed as a first-order reaction,

(25) O'Halloran, T. V.; Lippard, S. J. *J. Am. Chem. Soc.* **1983**, *105*, 3341.

(26) O'Halloran, T. V.; Lippard, S. J. *Inorg. Chem.* **1989**, *28*, 1289.

(27) Matsumoto, K.; Watanabe, T. *J. Am. Chem. Soc.* **1986**, *108*, 1308.

(28) Matsumoto, K.; Miyamae, H.; Moriyama, H. *Inorg. Chem.* **1989**, *28*, 2959.

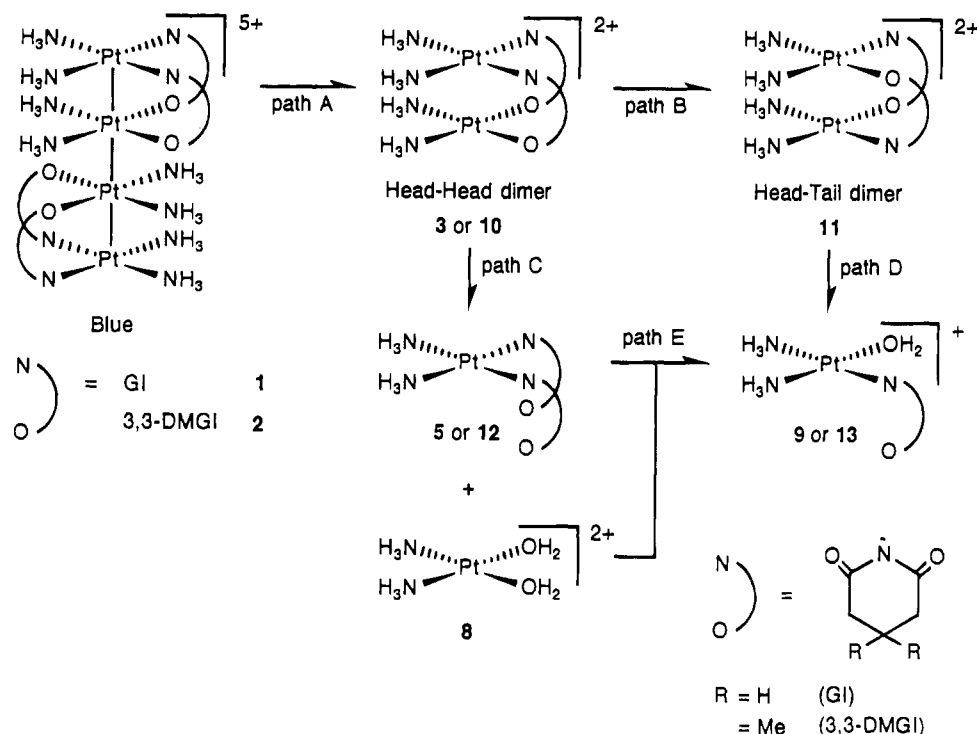
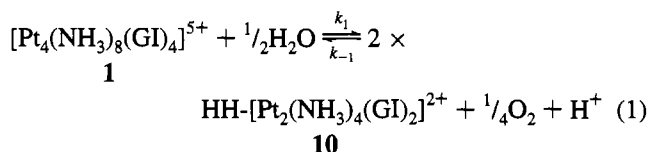
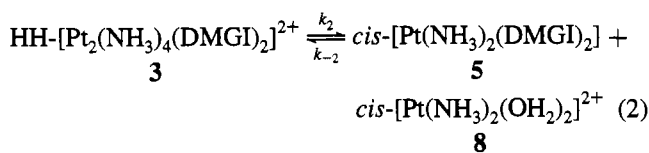


Figure 5. Solution behavior of 1 and 2 in H<sub>2</sub>O.



since the succeeding reactions and the reverse reaction of 1 are very slow compared to reaction 1. Although it was not possible to determine the reduction rate for 2, reduction of 2 is probably not slower than that of 1, since the redox potential of 2 (0.76 V vs SCE, determined with cyclic voltammetry) is higher than that of 1 (0.73 V vs SCE); therefore, 2 would be more easily reduced than 1.

The disruptive reaction of the HH dimer 3 into the monomers (path C) was followed with UV-vis spectroscopy as shown in Figure 6 for compound 3. The reaction is expressed as eq 2.



The spectra in Figure 6 show two isosbestic points at 237 and 263 nm, and the absorbance plot at 230 nm against time shows a simple first-order decay with the rate constant  $k_2$  of  $6.93 (2) \times 10^{-5} \text{ s}^{-1}$ . The reverse reaction  $k_{-2}$  or the succeeding reactions are slower compared to the forward reaction of eq 2.

From the reaction scheme in Figure 5, it seems that the antitumor activities of 1–3 would be exhibited by *cis*-[Pt(NH<sub>3</sub>)<sub>2</sub>(OH<sub>2</sub>)<sub>2</sub>]<sup>2+</sup> (8), which is also produced in the solution of *cis*-PtCl<sub>2</sub>(NH<sub>3</sub>)<sub>2</sub> and is now acknowledged as the real species reacting with DNA and exhibiting the antitumor activity.<sup>7–9</sup> The relatively weak coordination of the O atoms of DMGI and GI ligands facilitates reaction 2; thus, the HH dimers 3 and 10 or their oxidized tetranuclear forms 1 and 2 are antitumor active. The reaction rate  $k_2$  is almost comparable to the reported hydrolysis reaction rates of *cis*-DDP ( $9.5 \pm 1.3 \times 10^{-5} \text{ s}^{-1}$  in 3 mM NaCl and 1 mM NaH<sub>2</sub>PO<sub>4</sub>,<sup>34</sup> and  $7.6 \times 10^{-5} \text{ s}^{-1}$  in  $I = 0.318 \text{ M}$  with Na<sub>2</sub>SO<sub>4</sub><sup>35</sup>). This fact must also be responsible

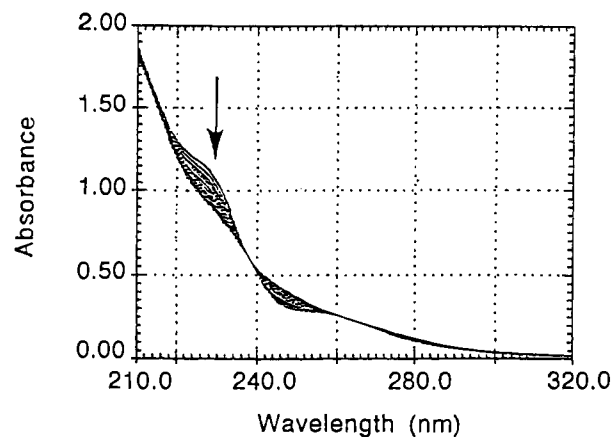
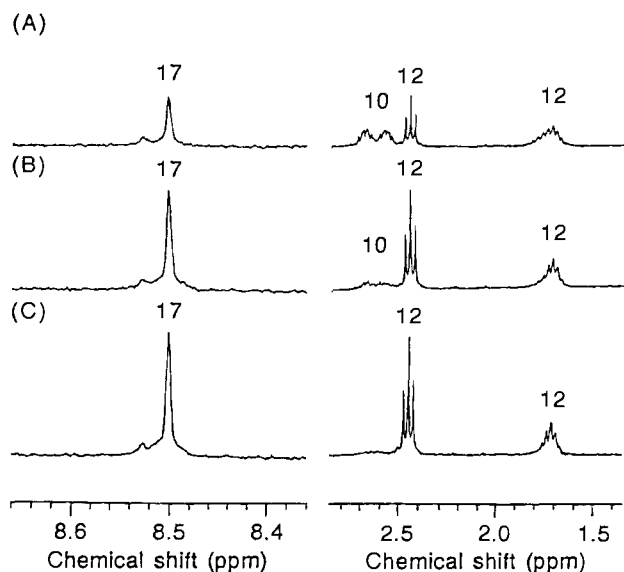


Figure 6. Spectral change of 3 (0.1 mM) in 0.01 M NaClO<sub>4</sub> aqueous solution at 37.0 °C. The spectrum was measured every 20 min.

Table 2. <sup>195</sup>Pt NMR Chemical Shifts Relative to K<sub>2</sub>PtCl<sub>4</sub> in D<sub>2</sub>O at -1624 ppm

| complex  | coordination environment | in H <sub>2</sub> O |          |                  |
|--|--------------------------|---------------------|----------|------------------|
|  |                          | L = GI              | L = DMGI | L = α-pyridonate |
| HH-[Pt <sub>2</sub> (NH <sub>3</sub> ) <sub>2</sub> L <sub>2</sub> ] <sup>2+</sup>             | N2O2                     | -1260               | -1259    | -1308            |
|  | N4                       | -2223               | -2233    | -2261            |
| HT-[Pt <sub>2</sub> (NH <sub>3</sub> ) <sub>2</sub> L <sub>2</sub> ] <sup>2+</sup>             | N3O                      | -1749               | -1754    | -1810            |
| <i>cis</i> -[Pt(NH <sub>3</sub> ) <sub>2</sub> (OH <sub>2</sub> ) <sub>2</sub> ] <sup>2+</sup> | N2O2                     | -1581               |          |                  |
| <i>cis</i> -[Pt(NH <sub>3</sub> ) <sub>2</sub> (OH <sub>2</sub> )L] <sup>+</sup>               | N3O                      | -1996               | -1988    | -2015            |
| <i>cis</i> -[Pt(NH <sub>3</sub> ) <sub>2</sub> L <sub>2</sub> ]                                | N4                       | -2408               | -2423    | -2495            |

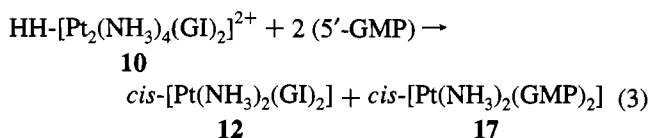
for the activities of 3 and 10, since reaction rate is known to be an important factor affecting the activity and the toxicity.<sup>6–8</sup> The <sup>195</sup>Pt NMR chemical shifts of each compound are listed in Table 2. Comparison of the <sup>195</sup>Pt NMR chemical shifts of the HH and HT dimers of GI, DMGI, and α-pyridonate (ref 23) clearly indicates that the Pt atoms receive less donation from GI or DMGI ligand than from α-pyridonate, and this explains the fact that the dimeric isomers of GI or DMGI ligand easily undergo solvolytic disruption to the monomers, whereas the corresponding α-pyridonate complex does not.



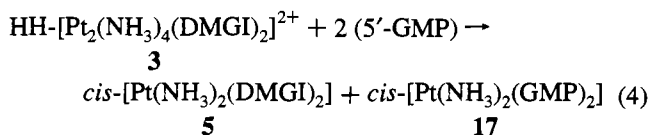
**Figure 7.**  $^1\text{H}$  NMR spectra of the reaction solution of **1** with 5'-GMP in  $\text{D}_2\text{O}$  at  $37.0\text{ }^\circ\text{C}$  with  $\text{pH} = 4$ ,  $[\text{Pt}] = 1\text{ mM}$ , and  $[5'\text{-GMP}] = 40\text{ mM}$ . (A) 0 min, (B) 77 min, (C) 155 min after the initiation of the reaction. The  $^1\text{H}$  chemical shift of **17** is 8.50 ppm.

#### Kinetic Study for the Reactions of the GI and DMGI Blue Complexes with 5'-Guanosinemonophosphate (5'-GMP).

Since it is known that guanine N7 position is the most favorable coordination site in DNA for platinum atoms in anticancer platinum complexes including *cis*- $\text{PtCl}_2(\text{NH}_3)_2$  in their reaction mechanism, the reaction of **1** with 5'-GMP was followed with  $^1\text{H}$  NMR and is shown in Figure 7. Dinuclear complex **10** is observed just after the reaction initiation; however, the peaks of the dimer decrease and at the same time the bis(GI) monomer **12** increases as the reaction proceeds. In the lower-field region where H8 of a guanine ring is observed, a new peak at 8.50 ppm appears besides the peak of free 5'-GMP (8.14 ppm). The new peak was assigned to *cis*- $[\text{Pt}(\text{NH}_3)_2(5'\text{-GMP})_2]$  (**17**), which was confirmed by comparison with the spectrum observed when a solution of **8** was mixed with excess 5'-GMP. The signal showed the same chemical shift and the same pH dependence. These spectral changes indicate that in the reaction with 5'-GMP, the reduced form of **1**, i.e. HH dimer **10** reacts with 5'-GMP to produce bis(GI) monomer **12** and bis(GMP) monomer **17** (eq 3).



The reaction of the reduced form of DMGI blue, i.e. HH dimer **3** with 5'-GMP was similarly carried out and the reaction was followed by  $^1\text{H}$  NMR spectroscopy (Figure S4). As the reaction proceeds, HH dimer **3** decreases, and bis(DMGI) monomer **5** and bis(GMP) monomer **17** are formed (eq 4).



Therefore, the reaction seems to be the same with GI blue **1**. Both the  $^1\text{H}$  NMR peak-height decrease of HH dimer **3** and the peak increase of bis(GMP) monomer **17** during the reaction with 5'-GMP obey first-order decay and increase, respectively (Figure S5), and the observed rate constants are  $k_{\text{obs}}(\mathbf{3}) = 2.91(5) \times$

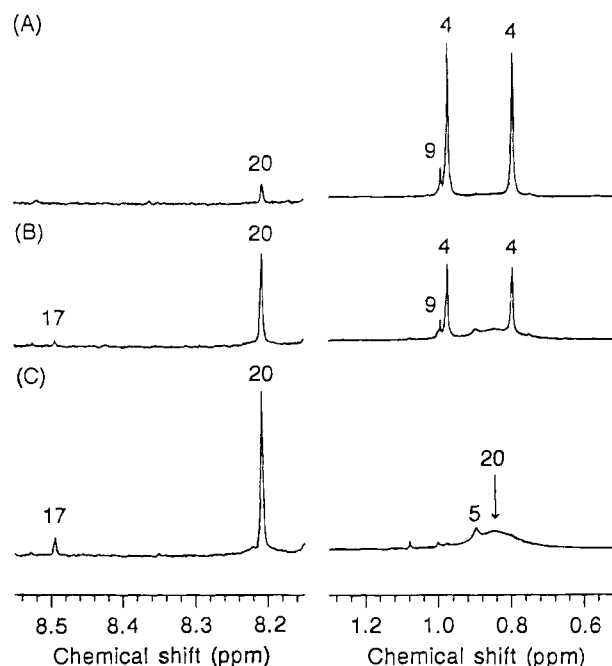
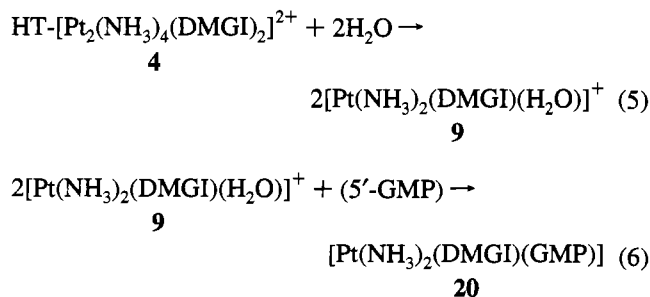


**Figure 8.**  $^1\text{H}$  NMR spectra of the aqueous reaction solution of  $\text{HT-}[\text{Pt}_2(\text{NH}_3)_4(\text{DMGI})_2]^{2+}$  (**4**) with 5'-GMP in  $\text{D}_2\text{O}$  at  $37.0\text{ }^\circ\text{C}$  with  $\text{pH} = 4$ ,  $[\text{Pt}] = 2\text{ mM}$ ,  $[\text{GMP}] = 20\text{ mM}$ . (A) 0 min, (B) 160 min, (C) 1088 min. The small peak at 1.08 ppm in C is free DMGI.

$10^{-4}\text{ s}^{-1}$  and  $k_{\text{obs}}(\mathbf{17}) = 2.80(13) \times 10^{-4}\text{ s}^{-1}$ . Therefore, the contribution of the intermediate reaction **3** and **17** would be, if at all, very little in the total reaction.

In the above reactions of the platinum complexes with 5'-GMP, all the coordination occurs at the N7 site of the guanine ring, which was confirmed by the conventional pH titration<sup>29,30</sup> by observing the H8 guanine proton NMR signal (Figure S6).

**The Reaction of Antitumor Inactive HT- $[\text{Pt}_2(\text{NH}_3)_4(\text{DMGI})_2]^{2+}$  (**4**) with 5'-GMP.** It is interesting and noteworthy that HT dimer is produced when GI blue **1** is dissolved in  $\text{H}_2\text{O}$  (Figure 4), while HT dimer is not directly observed in the corresponding DMGI HH dimer solution (Figure 3). It seems that for bulky DMGI ligand, isomerization of the HH and HT isomers is unfavorable. If HT dimer is produced in the solution of the blue complex, and both the HH and HT dimer themselves behave similarly to produce *cis*- $[\text{Pt}(\text{NH}_3)_2(\text{L})(\text{H}_2\text{O})]^+$  ( $\text{L} = \text{GI}$  or  $\text{DMGI}$ ) in solution as shown in Figure 5, the HT dimer would have antitumor activity. However, the screening test shows the opposite result (Table 1) at least for HT DMGI dimer **4**. In order to know how the HT dimer reacts with 5'-GMP, the reaction was followed by  $^1\text{H}$  NMR measurement. The spectra are shown in Figure 8, which shows that the following reactions take place.



(29) Admiraal, G.; Alink, M.; Altona, C.; Dijt, F. J.; van Garderen, C. J.; de Graaff, R. A. G.; Reedijk, J. *J. Am. Chem. Soc.* **1992**, *114*, 930.  
 (30) Bloemink, M. J.; Heetebrij, R. J.; Inagaki, K.; Kidani, Y.; Reedijk, J. *Inorg. Chem.* **1992**, *31*, 4656.

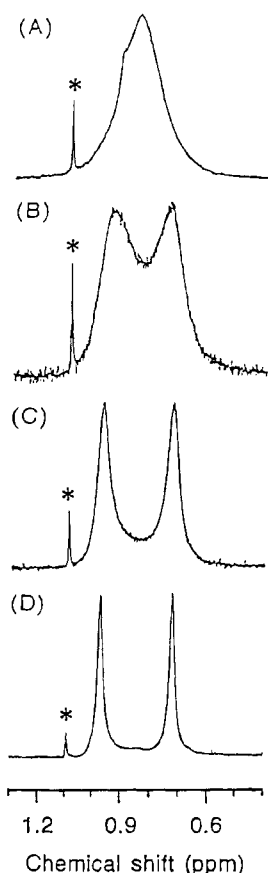


**Figure 9.** Variable temperature  $^1\text{H}$  NMR spectra of DMGI Me-H region of  $\text{cis-}[\text{Pt}(\text{NH}_3)_2(\text{DMGI})(\text{GMP})]$  (**20**). (A) 34 °C, (B) 24 °C, (C) 14 °C, (D) 4 °C. The peaks with an asterisk are free DMGI.

The solvolytic reaction of **4** to **9** has already been reported in  $\text{H}_2\text{O}$  and DMSO.<sup>17</sup> The reaction product of eq 6, i.e. compound **20** was reasonably identified from the broad signals of DMGI H2, H4, and Me-H (Figure 8) as explained in the following: These broad signals of the coordinated DMGI indicates that the free rotation around the Pt–N coordination bond becomes hindered by the coordination of a bulky ligand 5'-GMP in the adjacent *cis*-position. Variable-temperature measurement of the DMGI Me-H region of **20** (Figure 9) supports this assignment; the broad signals become sharp as the temperature is lowered to 4 °C, whereas the signals coalesce to a single peak at 34 °C. The coalescence temperature for **20** was 30.0 °C. Similar variable temperature measurement was done for analogous guanosine complex  $\text{cis-}[\text{Pt}(\text{NH}_3)_2(\text{DMGI})(\text{Guo})]^+$  (**22**) and the coalescence temperature was found to be 41.0 °C. From these data the activation energies for the free rotation of the coordinated ligands are  $60.6 \text{ kJ mol}^{-1}$  and  $63.1 \text{ kJ mol}^{-1}$  for **20** and **22**, respectively. It might be rather strange at first sight that less bulky guanosine complex shows higher activation energy than 5'-GMP complex, but this would suggest that the phosphate group of 5'-GMP is hydrogen-bonded to the ammine ligand, and therefore the ligand less hinders the free movement of DMGI.

From the  $^1\text{H}$  NMR measurement shown in Figures 8 and 9 it was found that HT dimer **4** does react with 5'-GMP and forms monosubstituted compound **20**, but the second substitution to the coordinated DMGI in **20** by 5'-GMP to produce **17** takes place only to a minor degree. The overall reaction is as follows: HT dimer **4** first disrupts to monomer **9**, whose aqua ligand is substituted by 5'-GMP to produce **20**. It seems that some of **9** loses DMGI ligand to produce **8** and free DMGI,

and a very small portion of **20** also loses DMGI to produce  $\text{cis-}[\text{Pt}(\text{NH}_3)_2(\text{GMP})(\text{H}_2\text{O})]^{2+}$  and free DMGI. Compound **9** reacts with free DMGI to become **5**. These reactions are exhibited in Figure 8. It is highly likely that the inability of HT dimer **4** to produce **17** is the origin of its antitumor inactive nature, although the compound is closely related to the antitumor active tetranuclear blue compound **2** and is produced in solution in the decomposition process of **2**. The  $^1\text{H}$  NMR data at 37 °C for the DMGI Me-H are; free DMGI, 1.08; compound **3**, 0.98 and 0.75; compound **11**, 0.98 and 0.80; compound **9**, 1.00; compound **5**, 0.90; compound **20**, 0.85(broad) ppm. The  $^1\text{H}$  NMR data for the G-H8 are; free 5'-GMP, 8.14; compound **20**, 8.21; **17**, 8.50 ppm.

It is also clear from the above facts that the coordinated DMGI in **20** is not a good leaving group for an antitumor drug.

Recently Hollis et al. reported that some mononuclear platinum complexes of the type  $\text{cis-}[\text{Pt}(\text{NH}_3)_2(\text{N-het})\text{Cl}]^+$  (N-het = N hetero-ring ligands) have antitumor activity,<sup>31</sup> and the first reaction occurring when the complexes are reacted with 5'-GMP is the formation of  $\text{cis-}[\text{Pt}(\text{NH}_3)_2(\text{N-het})(5'\text{-GMP})]^+$ ,<sup>32</sup> which is at present believed to be structurally responsible for the activity, but the study still needs detailed experiment to draw any conclusion on the relation of the activity and the structural type of the compound. Although compound **20** can be regarded similar to the  $\text{cis-}[\text{Pt}(\text{NH}_3)_2(\text{N-het})(5'\text{-GMP})]^+$  type compound, the precursor of **20**, i.e. HT dimer **4** is antitumor inactive.

## Conclusion

The present study has clarified how the structurally unstable tetranuclear blue compounds decompose to dimers and monomers in aqueous solution and how these solution behaviors affect the antitumor activity of the blue compounds. Those platinum blue compounds which produce monomeric diaqua complex **8** in solution, i.e. **1** and **2**, are antitumor active, whereas those which produce only HH and HT dimers, i.e. **6**<sup>33</sup> and **7**<sup>15</sup>, are inactive. Whether the tetranuclear structure disrupts only to dimers or further to monomers depends on the electron-donating degree of the bridging amidate ligand. DMGI and GI are weaker electron donors compared to  $\alpha$ -pyrrolidonate or acetamidate, because of the electron-withdrawing noncoordinating CO groups in the former ligands. It seems highly probable that the original antitumor activity of platinum pyrimidine blues<sup>9</sup> is also due to such disruptive reaction leading to the formation of diaqua complex **8**, considering the relatively weak donating nature of pyrimidines.

**Acknowledgment.** Financial support by Grant-in-Aids for Scientific Research on Priority Area of "Bioinorganic Chemistry" (03241101) from the Ministry of Education, Science and Culture, Japan, is gratefully acknowledged. The present study is a part of the Waseda University research project "Metal Coordination Complexes with Biological Activities".

**Supplementary Material Available:**  $^1\text{H}$  NMR spectra of **2** and **3** (Figure S1), the variable temperature  $^1\text{H}$  NMR spectra of **5** (Figure S2), UV-vis spectrum of **1** (Figure S3),  $^1\text{H}$  NMR spectra for the reaction of **3** with 5'-GMP (Figure S4),  $^1\text{H}$  NMR peak-height changes for **17** and **3** (Figure S5), and pH dependence of guanine H8 NMR chemical shifts (Figure S6) are available (6 pages). Ordering information is given on any current masthead page.

(31) Hollis, L. S.; Amundsen, A. R.; Stern, E. W. *J. Med. Chem.* **1989**, *32*, 128.

(32) Lempers, E. L. M.; Bloemink, M. J.; Brouwer, J.; Kidani, Y.; Reedijk, J. J. *Inorg. Biochem.* **1990**, *40*, 23.

(33) Matsumoto, K. *Inorg. Chim. Acta*, **1988**, *151*, 9.

(34) Bancroft, D. P.; Lepre, C. A.; Lippard, S. J. *J. Am. Chem. Soc.* **1990**, *112*, 6860.

(35) Reishus, J. W.; Martin, D. S., Jr. *J. Am. Chem. Soc.* **1961**, *83*, 2457.